Applied Catalysis B: Environmental 281 (2021) 119462

Contents lists available at ScienceDirect

Applied Catalysis B: Environmental

journal homepage: www.elsevier.com/locate/apcatb

HCN production from formaldehyde during the selective catalytic reduction of NO_x with NH_3 over V_2O_5/WO_3-TiO_2

Martin Elsener[a], Rob Jeremiah G. Nuguid[a,b], Oliver Kröcher[a,b], Davide Ferri[a,*]

[a] Paul Scherrer Institut, CH-5232 Villigen PSI, Switzerland
[b] Institute of Chemical Sciences and Engineering, École polytechnique fédérale de Lausanne (EPFL), CH-1015 Lausanne, Switzerland

ARTICLE INFO

Keywords:
HCN
Formaldehyde
SCR
V_2O_5/WO_3-TiO_2
TiO_2

ABSTRACT

Raw exhaust gases may contain notable levels of formaldehyde that can negatively impact the efficiency of after-treatment systems. In the selective catalytic reduction (SCR) of NO_x over V_2O_5/WO_3-TiO_2, formaldehyde was found to react with NH_3 to produce HCN at concentrations above the threshold limit value set by environmental/safety organizations. Due to this side reaction, NH_3 is consumed parasitically and the NO_x conversion decreases by up to 15 %, even after compensating for the fraction of lost NH_3. Under similar conditions, the non-reducible TiO_2 support also produced HCN moderately, thereby showing that redox sites promote the reaction but are not a necessary condition. To understand the chemistry responsible for HCN formation, the roles of reaction temperature, water, and oxygen were investigated. Our results suggest a new pathway for HCN production through the direct reaction of formaldehyde and NH_3, which is active at high temperature and does not proceed through the formate route previously proposed.

1. Introduction

The rise in anthropogenic nitrogen oxide (NO_x) emissions has impelled the development of exhaust after-treatment technologies. First introduced in the 1950's, the selective catalytic reduction (SCR) of NO_x by ammonia (NH_3) has enjoyed worldwide academic interest and industrial acceptance in the subsequent years. Because of its unparalleled efficiency, wide operating window, and moderate cost, SCR is the technology of choice for NOx reduction in Diesel-powered vehicles and thermal power plants [1–3].

More than 90 % of the NO_x emissions are in the form of nitric oxide (NO), and the main reaction taking place inside the reactor is the standard SCR reaction (Eq. 1).

$$4\ NO + 4\ NH_3 + O_2 \rightarrow 4\ N_2 + 6\ H_2O \quad (1)$$

The presence of nitrogen dioxide (NO_2) in the exhaust gas invokes the occurrence of the so-called fast SCR reaction (Eq. 2), wherein the reoxidation step of the metal center occurs much faster because of the stronger oxidizing power of NO_2 than oxygen (O_2) [4,5].

$$NO + NO_2 + 2\ NH_3 \rightarrow 2\ N_2 + 3\ H_2O \quad (2)$$

Besides the abatement of carbon monoxide (CO) and unburned hydrocarbons, Diesel oxidation catalysts (DOC) also partially oxidize NO to NO_2 and favor the fast SCR reaction [6].

The inherent complexity of the exhaust gas composition and gas-catalyst interactions can also promote side reactions during the SCR process. The most significant is the direct oxidation of NH_3 with O_2 (Eq. 3) [7,8].

$$4\ NH_3 + 3\ O_2 \rightarrow 2\ N_2 + 6\ H_2O \quad (3)$$

Although the major product of this parasitic reaction is nitrogen (N_2), NO can also form at high temperature, thereby negating the beneficial effect of NH_3 addition in the first place. Another undesirable side reaction is the formation of nitrous oxide (N_2O), a very potent greenhouse gas (Eq. 4). [9–11]

$$4\ NO + 4\ NH_3 + 3\ O_2 \rightarrow 4\ N_2O + 6\ H_2O \quad (4)$$

The extent of N_2O formation is catalyst-dependent, with Cu- and Fe-based SCR catalysts being more susceptible than V-based ones especially below 350 °C [12,13].

The production of hydrogen cyanide (HCN), a gas considered immediately dangerous to life, is another highly undesirable SCR side reaction. It was first observed over Cu-ZSM-5 when hydrocarbons were used as the reductant instead of NH_3 [14]. The extent of HCN formation followed a volcano-shaped profile with temperature, and the activity depended on the type of hydrocarbon used. With ethene and propene,

* Corresponding author.
E-mail address: davide.ferri@psi.ch (D. Ferri).

https://doi.org/10.1016/j.apcatb.2020.119462
Received 10 July 2020; Received in revised form 18 August 2020; Accepted 20 August 2020
Available online 22 August 2020
0926-3373/ © 2020 The Authors. Published by Elsevier B.V. This is an open access article under the CC BY license (http://creativecommons.org/licenses/by/4.0/).

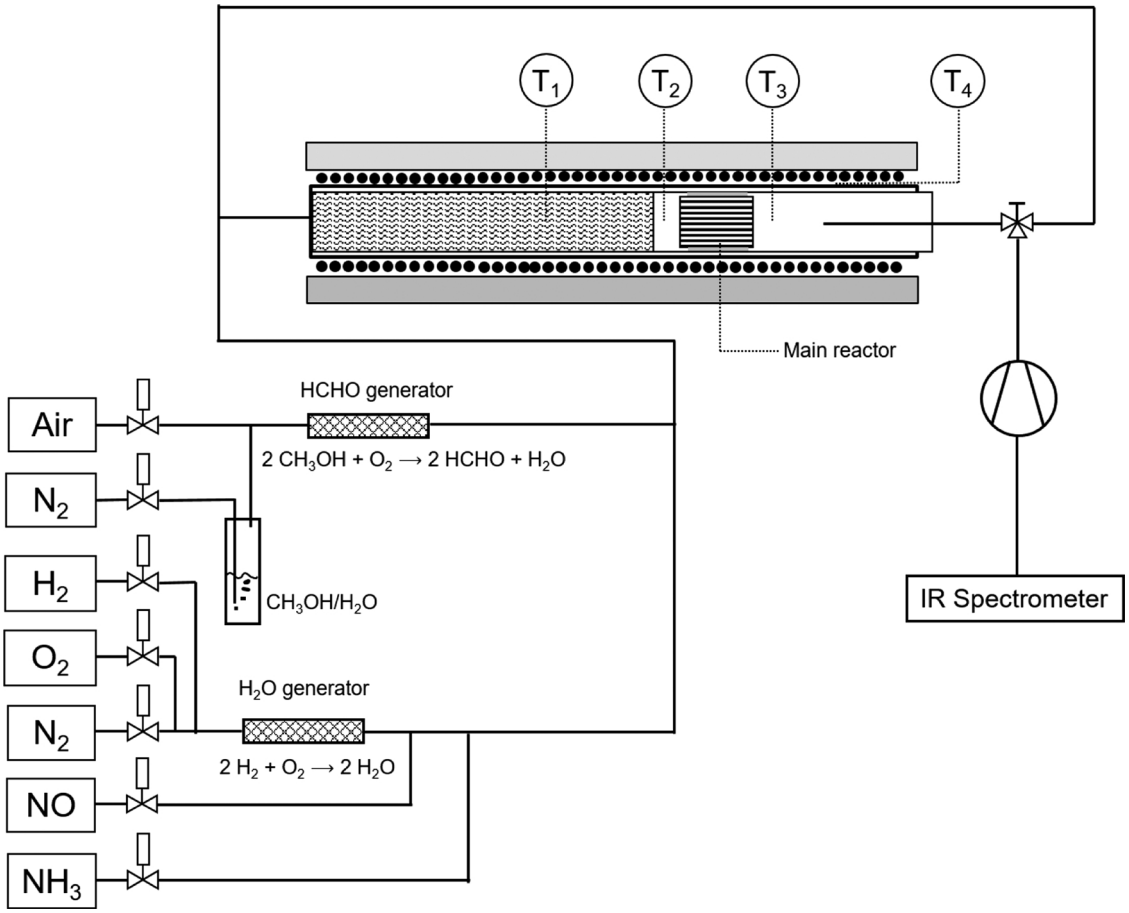

Fig. 1. Experimental set-up with the mass flow controllers, H_2O generator, HCHO generator, main reactor, heating system, and IR spectrometer for gas analysis.

the HCN concentration reached a maximum value at 325 and 225 °C, respectively. The presence of water in the feed generally increased the amount of HCN produced [15]. It became evident that HCN formation did not solely apply to Cu-ZSM-5, but also to other catalysts operating under hydrocarbon-SCR [16–19].

HCN was also observed during NH_3-SCR. When ammonium formate decomposition is exploited to generate NH_3 instead of urea, it should ideally decompose according to Eq. 5 [20].

$$HCOONH_4 \rightleftharpoons NH_3 + HCOOH \quad (5)$$

As this is an endothermic reaction ($\Delta_r H^\circ = 85\ kJ{\cdot}mol^{-1}$), the equilibrium shifts in favor of ammonium formate at low temperature. This can give rise to another decomposition pathway in which it undergoes subsequent dehydration steps to form formamide (Eq. 6) and eventually HCN (Eq. 7).

$$HCOONH_4 \rightleftharpoons HCONH_2 + H_2O \quad (6)$$

$$HCONH_2 \rightleftharpoons HCN + H_2O \quad (7)$$

Both formamide and HCN were observed below 250 °C under SCR-relevant conditions, and the decrease in HCN production correlated well with the increase of SCR activity. As more NH_3 was consumed to satisfy the increased NO_x reduction at higher temperatures, more ammonium formate was decomposed according to Eq. 5, thereby rendering Eq. 6 and Eq. 7 less probable. Nonetheless, this reaction path showed very low HCN yield. A very recent study proposed that a similar route was responsible for HCN production under NH_3-SCR conditions in the presence of formaldehyde (HCHO) [21]. Formed due to the incomplete oxidation of hydrocarbons, formaldehyde is a noxious compound that is nominally present as a trace constituent in the exhaust of internal combustion engines [22–25]. This is particularly problematic for stationary natural gas engines, which usually do not operate an oxidation catalyst upstream of the SCR catalyst. The unwanted side reaction between formaldehyde and NH_3 can potentially lower NO_x conversion by consuming NH_3 that is otherwise reserved for SCR. While the decrease in SCR activity is certainly detrimental, the major problem really stems from the high toxicity of the produced HCN. The European Commission set the maximum occupational exposure limit of HCN at only 0.9 ppm. Hence, the release of even minute quantities of HCN to the environment can have grave consequences for air quality and human health [26,27]. It is therefore imperative to investigate this side reaction in detail to develop potential measures for mitigation.

In this study, we show that formaldehyde reacts with NH_3 to form HCN with high yields under SCR conditions, and that the reaction does not require the formation of ammonium formate.

2. Materials and methods

2.1. Materials

The catalyst in this study comprised of 2 wt% V_2O_5/WO_3-TiO_2 that was prepared by wet impregnation. A sufficient amount of ammonium metavanadate (NH_4VO_3; Fluka, > 99.0%) was dissolved in water at 60 °C, and was mixed with 10 wt% WO_3/TiO_2 (DT-52, Cristal) for 1 h. After removal of water under reduced pressure, the sample was calcined in a muffle furnace at 550 °C for 10 h. The resulting surface area of the calcined catalyst is ~90 $m^2\,g^{-1}$, which does not vary significantly from that of the starting 10 wt% WO_3/TiO_2 material. [28] At this relatively low loading and calcination temperature, V_2O_5 and WO_3 are well-dispersed and only reflections from anatase could be detected by x-ray

diffraction. [28–30] For comparative purposes, TiO_2 (DT-51, Cristal; ~100 $m^2 g^{-1}$) was also used without additional modification.

Cordierite honeycomb monoliths (Corning, 400 cpsi, 17 mm x 12 mm x 50 mm) were repeatedly immersed in an aqueous slurry of V_2O_5/WO_3-TiO_2 or TiO_2 and then dried in air to achieve a loading of 130 g·L^{-1} of material. The washcoated monoliths were dried and then calcined in a muffle furnace at 500 °C for 5 h.

2.2. Catalytic measurements

The measurements were carried out in a custom-built model gas test bench (Fig. 1). Mass flow controllers (MFCs) were used to regulate the flows of air, N_2 (99.999 vol%, Air Liquide), H_2 (99.998 vol%, Air Liquide), O_2 (99.998 vol%, Air Liquide), NO (6 vol% in N_2, Air Liquide), and NH_3 (4 vol% in N_2, Air Liquide). Water was generated in situ from the reaction of H_2 and O_2 through a Pt-based catalyst (H_2O generator), which is preferred over conventional water vaporization as it allows for a pulsation-free water feed.

Formaldehyde was generated in situ through the partial oxidation of methanol over V_2O_5/WO_3-TiO_2 (200 − 500 µm) in a separate stainless steel reactor (HCHO generator). For this purpose, N_2 was bubbled through a 50 vol% aqueous solution of methanol at ambient temperature before mixing with air and flowing through the catalyst bed heated at 250 °C to produce 150 ppm formaldehyde. Under these conditions, methanol oxidation was not complete, and the feed to the main reactor contained also 10 − 15 ppm methanol, ~1 ppm formic acid, ~350 ppm CO, and 0.1 − 0.2 vol% H_2O. All gas lines were heated to 150 °C to prevent the condensation of components with low vapor pressure.

The model gas (GHSV = 50,000 h^{-1}) consisted of 10 vol% H_2O and 10 vol% O_2 balanced in N_2 with variable amounts of formaldehyde, NO, and NH_3 as indicated in Table 1.

In most SCR catalytic studies, NH_3 and NO_x are dosed at the same concentration across the temperature range under study. This technique is often sufficient to compare catalysts with different activities. However, for practice-relevant measurements, it is more useful to determine the NO_x conversion by varying the NH_3 dosage until a defined NH_3 slip occurs (usually 10 ppm) [31]. For this purpose, the catalyst in this study was exposed to a constant feed of NO_x and increasing dosages of NH_3 at a given temperature until the outlet concentration is ~10 ppm. All of the NH_3 dosages as well as outlet concentrations of NO and NH_3 are reported in Table S-1.

The effects of O_2 and water on HCN formation were also investigated. The O_2 content was varied from 2.5 to 15 vol% in a gas feed containing 10 vol% H_2O, 150 ppm formaldehyde, and 300 ppm NH_3. In a similar way, the water content was changed from 0 to 12.5 vol% in a gas feed containing 10 vol% O_2, 150 ppm formaldehyde, and 300 ppm NH_3.

For comparison, formic acid was also dosed in the reactor instead of formaldehyde by bubbling N_2 through a 30 vol% aqueous solution of formic acid at ambient temperature. The HCHO generator was bypassed in order to prevent any subsequent oxidation of formic acid prior to meeting the catalyst in the main reactor. This resulted in 150 ppm formic acid in the feed.

The main reactor (quartz glass tube; d_{int} = 28 mm) had three heating zones, including the preheating zone (T_1), which was filled with ceramic beads to avoid radial temperature gradients of the model gas feed. Thermocouples inserted in the center of the quartz tube before (T_2) and after the catalyst module (T_3) ensured uniform temperature control of the catalyst bed. The temperature of the reactor outlet was measured and controlled via the thermocouple (T_4) installed on the outer wall of the reactor. After being wrapped in ceramic fiber paper, the washcoated monolith piece was inserted in the rectangular opening of a cylindrical stainless steel holder that was itself wrapped with ceramic fiber paper for sealing against the reactor wall.

The outlet of the main reactor and the bypass line were connected to a gas feed pump (KNF) that was heated at 170 °C. A manual three-way valve allowed the gas from either the reactor or the bypass line to pass through a 2-m gas cell mounted in the sample compartment of a Nexus Fourier transform infrared spectrometer (Thermo-Nicolet) and heated at 180 °C. The gas components were quantified using the Omnic/Quantpad software. The acquisition time was 8 s per measurement point (average of 4 spectra). To obtain the lowest possible detection limit (DL), a total of 10 measurement points were averaged. Typical DL values ranged from 0.2 to 1 ppm (Table S-2).

The degree of NO_x conversion was calculated according to Eq. 8.

$$NO_x\ conversion = \frac{[NO]_{in} - [NO_x]_{out}}{[NO]_{in}} \cdot 100\% \quad (8)$$

where $[NO]_{in}$ and $[NO_x]_{out}$ are the concentration of NO in the gas feed, and the concentration sum of NO and NO_2 after the reactor, respectively.

As mentioned previously, the oxidation of methanol in the HCHO generator was not complete and left 10 − 15 ppm methanol in the feed to the main reactor. This unreacted fraction could potentially be oxidized once it passes through the catalyst sample. Hence, the formaldehyde conversion was calculated according to Eq. 9 to account for the unreacted methanol.

$$HCHO\ conversion = \left(1 - \frac{[HCHO]_{out}}{[HCHO]_{in} + [CH_3OH]_{in}}\right) \cdot 100\% \quad (9)$$

where $[HCHO]_{out}$, $[HCHO]_{in}$, and $[CH_3OH]_{in}$ are the concentrations of formaldehyde after the reactor, formaldehyde in the gas feed, and methanol in the gas feed, respectively.

The HCN yield from formaldehyde is defined according to Eq. 10.

$$HCN\ yield = \frac{[HCN]_{out}}{[HCHO]_{in} + [CH_3OH]_{in}} \quad (10)$$

where $[HCN]_{out}$, $[HCHO]_{in}$, and $[CH_3OH]_{in}$ are the concentrations of HCN after the reactor, formaldehyde in the gas feed, and methanol in the gas feed, respectively.

Aside from HCN, other products can also form from formaldehyde, with CO and CO_2 (CO_x) being the most notable. Hence, the selectivity of formaldehyde consumption toward the formation of HCN and CO_x is given by Eq. 11 and Eq. 12.

$$HCN\ selectivity = \frac{[HCN]_{out}}{[HCN]_{out} + [CO_x]_{out}} \quad (11)$$

$$CO_x\ selectivity = \frac{[CO_x]_{out}}{[HCN]_{out} + [CO_x]_{out}} \quad (12)$$

where $[HCN]_{out}$ and $[CO_x]_{out}$ are the concentration of HCN after the reactor and the concentration sum of CO and CO_2 after the reactor, respectively.

Table 1
Feed conditions employed in the study.

Feed label and composition	Formaldehyde (ppm)	NO (ppm)	NH_3 (ppm)
SCR feed ($NH_3/NO/H_2O/O_2/N_2$)	0	300	Required concentration to achieve ~10 ppm NH_3 slip
HCHO feed ($HCHO/H_2O/O_2/N_2$)	150	0	0
HCHO + SCR feed ($HCHO/NH_3/NO/H_2O/O_2/N_2$)	150	300	Same concentration as in "SCR feed"
HCHO + adj. SCR feed (HCHO/adj. $NH_3/NO/H_2O/O_2/N_2$)	150	300	Required concentration to achieve ~10 ppm NH_3 slip

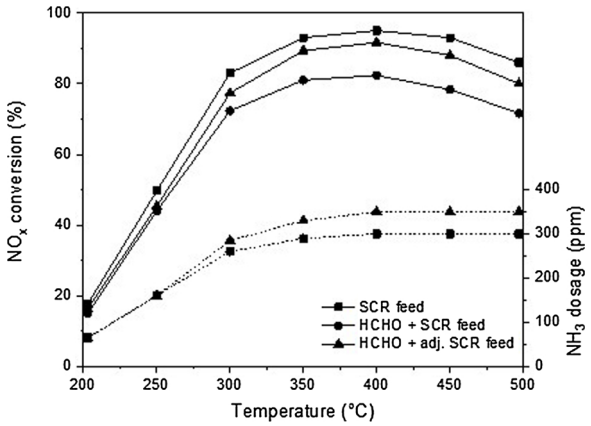

Fig. 2. NO conversion over V_2O_5/WO_3-TiO_2 at 10 ppm NH_3 slip in the presence and absence of formaldehyde and the corresponding NH_3 dosage (experimental conditions listed in Table 1 and Table S-2). The NH_3 dosages for SCR feed and HCHO + SCR feed are the same and therefore the respective curves perfectly overlap. Dotted lines refer to the NH_3 dosage.

3. Results and discussion

3.1. Influence of HCHO on the SCR reaction

Fig. 2 shows the NO conversion obtained at 10 ppm NH_3 slip over V_2O_5/WO_3-TiO_2 and the actual amount of NH_3 dosed. The performance of V_2O_5/WO_3-TiO_2 in the absence of formaldehyde (Fig. 2; SCR feed) was comparable with those reported in the literature for the same V loading and GHSV [28,30]. Regardless of the conditions applied, the trends followed a similar profile. The NO_x conversion increased between 200 and 300 °C, and passed through a maximum value between 350 and 400 °C. Two factors can contribute to the decrease in the NO_x conversion above 450 °C: the direct oxidation of NH_3 that becomes increasingly favorable at high temperature and the decreased amount of NH_3 on the catalyst surface due to decreased adsorption.

The presence of formaldehyde had a negative effect on the NO_x conversion at the same NH_3 dosage (Fig. 2; HCHO + SCR feed). As an illustration, nearly 95% of the NO_x in the gas feed could be abated with 300 ppm NH_3 at 400 °C in the absence of formaldehyde, but this value dropped to 82% with formaldehyde. The decrease in the catalytic performance could be attributed to the depletion of the available NH_3 for SCR as it is consumed in the presence of formaldehyde.

At low temperatures, a lower NH_3 dosage was necessary to achieve 10 ppm of NH_3 slip because the catalytic activity was rather limited. Correspondingly, the NO_x conversion was not affected significantly by the presence of formaldehyde, with less than 5% of catalytic performance being lost due to the introduction of formaldehyde at 250 °C. Although NH_3 could react with formaldehyde, it was still preferentially consumed by SCR. Hence, formaldehyde competed with NO_x for reaction with NH_3 only when the temperature was sufficiently high (i.e., above 300 °C). These results imply that the activation energy for the side reaction is much higher than that of the SCR reaction.

To further investigate the effect of formaldehyde on the SCR reaction, the NH_3 dosage was readjusted to meet the 10 ppm slip NH_3 (i.e., compensation for the amount of NH_3 lost in the side reaction). As more NH_3 became available for SCR, the NO_x conversion increased, but did not return to the original value obtained in the absence of formaldehyde. When the NH_3 dosage was adjusted from 300 to 350 ppm at 400 °C, the NO_x conversion increased from 82% to 92%, but not to the initial 95% obtained in the absence of formaldehyde. This behavior implies that the side reaction consuming formaldehyde could take place at the same catalytic sites responsible for SCR.

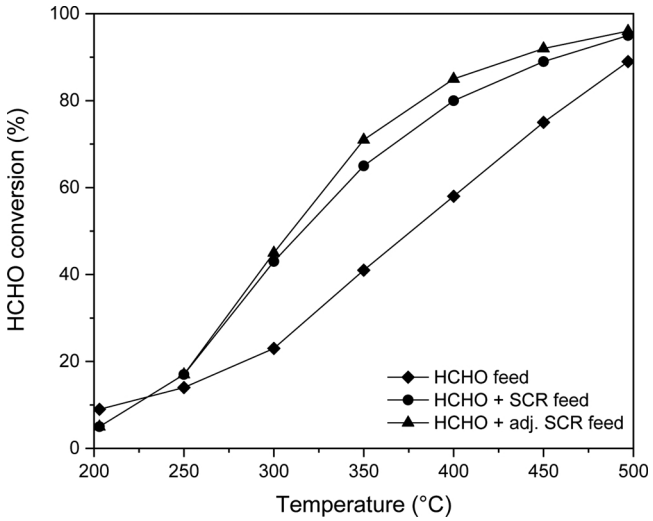

Fig. 3. Formaldehyde conversion over V_2O_5/WO_3-TiO_2 in the presence and absence of SCR (experimental conditions listed in Table 1 and Table S-1).

3.2. Formaldehyde conversion

Fig. 3 shows the formaldehyde conversion over the same catalyst. Under a purely oxidative atmosphere (Fig. 3; HCHO feed), formaldehyde conversion increased from 9% to 89% as the temperature was varied from 200 to 500 °C. CO was the major product observed, which reflects the oxidation activity of V_2O_5/WO_3-TiO_2 catalysts. At 200 °C, traces of formic acid were also detected in the gas phase. This suggests that formic acid formation is the first reaction step of formaldehyde oxidation. Indeed, previous infrared spectroscopic studies have shown that surface formate species were formed almost instantaneously upon introduction of formaldehyde, and that they prevailed over surface formaldehyde species [32,33]. Nonetheless, formates do not desorb as formic acid significantly, suggesting that the formed surface species are reaction intermediates. Above 450 °C, traces of CO_2 were also observed in the gas phase.

Formaldehyde conversion generally increased under SCR conditions (Fig. 3; HCHO + SCR feed). The only exception was at 200 °C where it was slightly lower (5% vs. 9%), indicating that NH_3 probably inhibits the oxidation of formaldehyde at low temperature. As the temperature increased, more formaldehyde was consumed in presence of the SCR feed. The maximum difference of 24 % in formaldehyde conversion between the two feed conditions was recorded at 350 °C. This behavior suggests that formaldehyde reacted with NH_3. At 500 °C, the two formaldehyde conversion levels were again very close. It is important to note that addition of 300 ppm NO in the absence of NH_3 (Table S-3) did not cause any change in formaldehyde conversion, demonstrating that NO is not involved in side reactions with formaldehyde.

When the NH_3 feed was adjusted to meet 10 ppm NH_3 slip (Fig. 3; HCHO + adj. SCR feed), the formaldehyde conversion improved particularly in the temperature regime between 300 and 500 °C, indicating that the side reaction was further promoted by the increased NH_3 dosage. Hence, an increase in NH_3 concentration increases NO_x conversion but promotes simultaneously the side reaction of NH_3, effectively subtracting NH_3 from the main SCR reaction pathway.

Under similar conditions, TiO_2 was also able to oxidize formaldehyde to some degree, reaching 15 % and 25 % conversion at 500 °C in the absence and presence of NH_3, respectively (Figure S-1). Formaldehyde conversion was low likely because TiO_2 did not have appreciable redox activity in the temperature range studied.

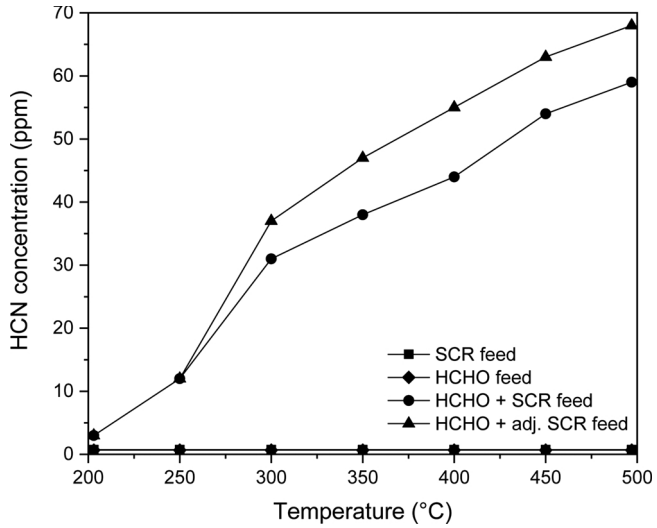

Fig. 4. HCN formation at 10 ppm NH_3 slip over V_2O_5/WO_3-TiO_2 (experimental conditions listed in Table 1 and Table S-2). The HCN concentrations for SCR feed and HCHO feed are the same and the respective curves therefore perfectly overlap.

3.3. Formation of HCN

Fig. 4 shows the concentration of HCN formed as a function of temperature in the same experiment presented in Fig. 2 and Fig. 3. In the absence of either formaldehyde or NH_3, no HCN was observed (Fig. 3; SCR feed and HCHO feed).

When formaldehyde and NH_3 were fed simultaneously, the HCN concentration increased from 3 to 59 ppm as the temperature was raised from 200 to 500 °C (Fig. 4; HCHO + SCR feed). The steepest rise occurred between 250 and 300 °C, where the HCN concentration more than tripled.

When the NH_3 dosage was adjusted to meet the 10 ppm slip, even more HCN was produced (Fig. 4; HCHO + adj. SCR feed). For example, HCN increased from 44 to 55 ppm when the NH_3 supply was changed from 300 to 350 ppm. This explains why the NO_x conversion reported in Fig. 2 did not reach the same levels in the absence of formaldehyde, even if additional NH_3 was supplied. HCN production is therefore confirmed to be in direct competition with SCR, especially at high temperatures.

Even a non-reducible material such as TiO_2 showed mild HCN formation under similar conditions, the HCN concentration varying from 2 ppm at 350 °C to 11 ppm at 500 °C (Figure S-2). While the presence of redox-active sites such as VO_x increases HCN production significantly, the metal oxide support already provides a non-negligible baseline activity.

HCN formation over V_2O_5/WO_3-TiO_2 was strongly temperature-dependent, but it remained constant when the O_2 content was varied from 2.5 to 15.0 vol% (Figure S-3). This suggests that excess O_2 does not cause the side reaction to stop in favor of the direct oxidation of formaldehyde. In fact, formaldehyde conversion and CO_x formation were also found to be independent of O_2 content.

In contrast, water had a significant impact on HCN production. Formaldehyde conversion decreased from 99 % to 89 % as the water concentration increased from 0 to 12.5 vol% (Fig. 5). This might be due to the co-adsorption of water on the catalyst, which is also known to inhibit the SCR reaction by decreasing the adsorption sites for NH_3, among other effects [34].

HCN selectivity also decreased similar to formaldehyde conversion, which suggests that formaldehyde requires close proximity with the active sites for HCN production. However, CO_x selectivity followed an opposite trend. Without water, CO_x formation was negligible, but CO_x

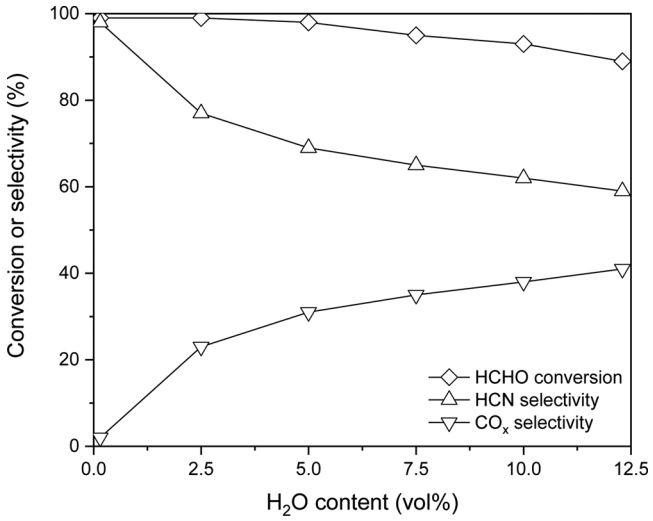

Fig. 5. Effect of water content on the formaldehyde conversion, HCN selectivity, and CO_x selectivity over V_2O_5/WO_3-TiO_2 at 350 °C.

selectivity increased to 41 % at the highest water level investigated in the study. Water could transform formaldehyde into adsorbed formate species [32,33], which were already proposed to be intermediates for CO_x formation in the previous sections. The positive effect of water on CO_x formation further confirms this pathway. The same strong effect of water was observed also on TiO_2. In the absence of water, 111 ppm HCN were produced from reaction of formaldehyde and NH_3 at 500 °C with practically full conversion of formaldehyde, while only 11 ppm HCN and 25 % formaldehyde conversion were observed with 10 vol% H_2O (Figure S-4).

The increase in water concentration and the subsequent formation of formate species appeared to be detrimental for HCN formation, suggesting that it follows a different mechanism than CO_x formation. To confirm that formate species were not relevant for HCN formation, formic acid was dosed together with NH_3 over V_2O_5/WO_3-TiO_2 (Fig. 6). Similar to the case of formaldehyde, HCN formation from formic acid was also negatively affected by the presence of water. Under 10 vol% H_2O – which is the usual water content in exhaust gas and the same condition applied in the measurements presented in Fig. 4 – HCN did not form in significant amounts; all of the measurements fell below the detection limit of 1 ppm. Even when the water content was decreased to 5 vol%, no HCN was observed. In fact, it is only in the absence of water

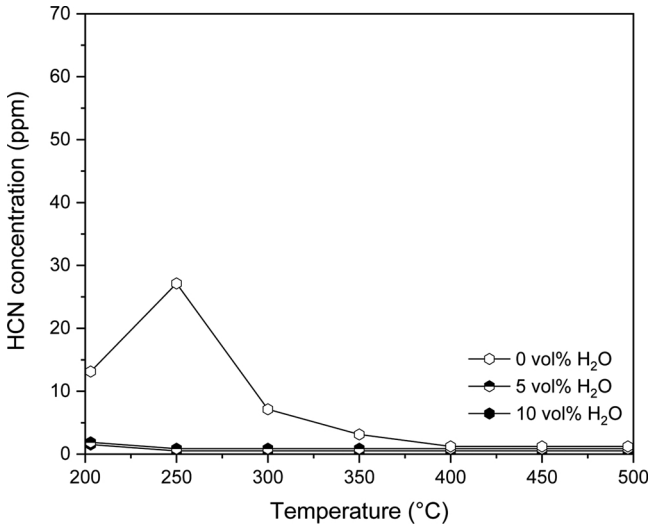

Fig. 6. HCN formation from formic acid over V_2O_5/WO_3-TiO_2.

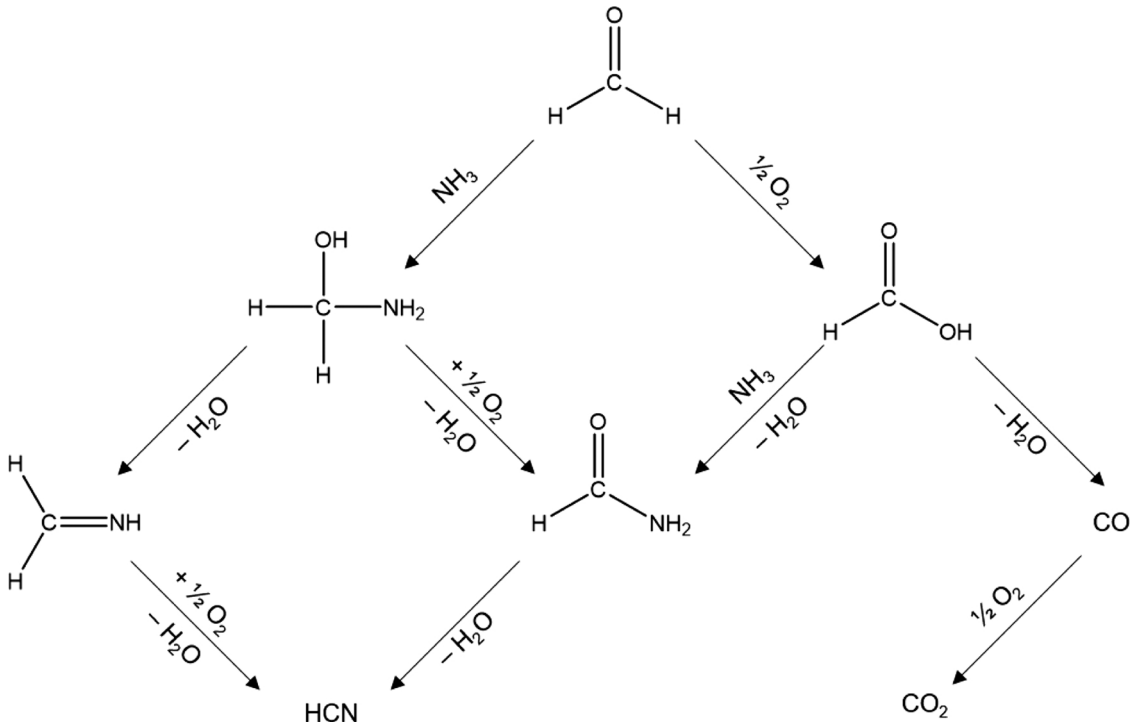

Fig. 7. Proposed reaction pathway of HCN formation.

that formic acid formed HCN, but in rather limited amounts compare to the case of formaldehyde. This proves that HCN formation from formaldehyde cannot proceed through the formate route; instead, HCN more likely originates from the direct reaction of formaldehyde with NH_3.

Finally, it is important to note that HCN formation from formaldehyde and formic acid followed different behaviors with temperature. Whereas HCN formation increased continuously with temperature when formaldehyde was the reactant (Fig. 4), it experienced a maximum at 250 °C and then decreased rapidly when formic acid was used instead (Fig. 6). This is the same behavior observed in a previous study where ammonium formate was used as a reducing agent for SCR [20]. Hence, this confirms that two different mechanisms are responsible for HCN formation depending on the carbonyl precursor: a high-yielding route with formaldehyde that is active above 300 °C and a moderate one with formic acid that operates only below 300 °C.

3.4. Proposed reaction pathway

Based on the discussed experimental pieces of evidence, we propose the new reaction pathway for the formation of HCN over V_2O_5/WO_3-TiO_2 in Fig. 7.

3.4.1. Oxidation of formaldehyde

When formaldehyde adsorbs onto the catalyst, it can readily transform into formate species due to the oxidizing atmosphere of the gas feed and the catalyst surface. This oxidative transformation occurs also over TiO_2 [32,33]. Indeed, some traces of the formate species can desorb as formic acid, which was detected in trace amounts at low temperature.

Formation of formic acid might also be possible through the Cannizzaro reaction [35], a base-catalyzed process resulting in the disproportionation of formaldehyde to methanol and formic acid, according to Eq. 13.

$$2\ HCHO\ +\ H_2O \rightarrow CH_3OH\ +\ HCOOH \quad (13)$$

This reaction occurred over TiO_2 under 0.1 – 0.2 vol% H_2O, and methanol was detected between 200 and 350 °C (Figure S-5). On the contrary, no methanol was observed over V_2O_5/WO_3-TiO_2, suggesting that Eq. 13 does not contribute significantly to formic acid formation in the presence of redox-active sites. Hence, the direct oxidation of formaldehyde is proposed as the major route for formic acid production in this study.

Formate species are short-lived, and are quickly oxidized into CO in a subsequent step (Fig. 7). Previous studies have shown that formic acid decomposes readily in the temperature range of 180 – 250 °C [36–38]. This is in line with our catalytic measurements showing traces of formic acid only at 200 °C, the lowest temperature investigated. However, CO was the major product of formaldehyde oxidation over V_2O_5/WO_3-TiO_2 and only small amounts of CO_2 were detected at 500 °C.

Detection of low levels of H_2 above 350 °C in the absence of water over TiO_2 confirms that formaldehyde decomposes also into CO and H_2 (Figure S-5), but not over V_2O_5/WO_3-TiO_2.

3.4.2. Formation of HCN through formic acid and NH_3

The formed formic acid could then react with NH_3 to yield ammonium formate, which is the reverse of Eq. 5. In this situation, HCN is formed after two successive dehydration steps (Eqs. 6 and 7). This is the same route that was previously proposed for HCN production when ammonium formate was used as the NH_3 precursor instead of urea [20].

Our catalytic measurements with formic acid revealed that this route is only possible at low temperature, reaching maximum activity at 250 °C (Fig. 6). At higher temperatures, the direct decomposition of formic acid into CO and water becomes more favorable. Under these conditions, Eq. 5 also shifts toward the formation of formic acid and NH_3 and as a result, less ammonium formate and HCN can be formed. Furthermore, this route is strongly inhibited by the presence of water (Fig. 6). Hence, this reaction pathway cannot explain the high amounts of HCN observed at high temperatures and considerable amounts of water.

3.4.3. Formation of HCN through the direct reaction of formaldehyde and NH_3

Based on the above considerations, we propose that under the

conditions used in the study, formaldehyde and NH_3 react with each other to form HCN. The preference for this reaction can be derived from known chemical reactions. The carbonyl carbon of formaldehyde is susceptible to nucleophilic attack by NH_3, yielding methanolamine (Equation 14) [39], which is analogous to the reaction of aldehydes with water to form a geminal-diol or with an alcohol to form a hemiacetal [40,41].

$$HCHO + NH_3 \rightleftharpoons HO\text{-}CH_2\text{-}NH_2 \quad (14)$$

Methanolamine can undergo two dehydration pathways that both ultimately lead to the production of HCN. The first one is oxidative dehydration, which requires at least a mild oxidation catalyst. Because of the excess O_2 in the feed and the fact that VO_x supported on TiO_2 possesses oxidation activity [42], methanolamine can easily transform into formamide (Equation 15).

$$HO\text{-}CH_2\text{-}NH_2 + ½\ O_2 \rightleftharpoons HCONH_2 + H_2O \quad (15)$$

Formamide dehydrates to form HCN in an endothermic reaction ($\Delta_r H^\circ = 140\ kJ{\cdot}mol^{-1}$) according to Eq. 16. This reaction pathway is in agreement with the high levels of HCN observed as the temperature was increased.

$$HCONH_2 \rightleftharpoons HCN + H_2O \quad (16)$$

The two intermediates, methanolamine and formamide, were not observed in this study and are thus supposed to be formed and consumed at the surface of the catalyst. It is also important to mention that this final dehydration step is shared with the reaction pathway starting from formic acid (Eq. 6 and Eq. 7). However, formic acid is very easily oxidized to CO, thus formamide is not formed in the first place.

The second possible dehydration pathway follows the Strecker synthesis of amino acids [43]. According to this reaction, methanolamine decomposes into methanimine and water, as confirmed by calculations (Eq. 17) [44].

$$HO\text{-}CH_2\text{-}NH_2 \rightleftharpoons CH_2NH + H_2O \quad (17)$$

Methanimine is a highly unstable molecule [45,46] and is therefore not detected as a product even at low temperatures. Instead, it can oxidize rapidly on the catalyst surface to yield HCN and water (Eq. 18).

$$CH_2NH + ½\ O_2 \rightleftharpoons HCN + H_2O \quad (18)$$

3.5. Practical relevance

HCN forms under SCR conditions in the temperature range of $200-500\ ^\circ C$. This side reaction is highly undesired because of two reasons. First, HCN is a poisonous gas that harms human health and the environment. Second, the side reaction leading to HCN formation not only consumes NH_3 parasitically, but also retards SCR activity by up to 20 % (Figure S-6). This means that a larger catalyst bed or monolith brick would be needed to achieve the same reactivity in the absence of formaldehyde.

Formaldehyde and other potential carbonyl species in the gas feed result from the partial oxidation of hydrocarbons. Hence, these species must be fully oxidized to avoid potential side reactions before passing through the SCR catalyst compartment. For mobile systems, this is not really an issue because oxidation catalysts and NH_3 slip catalysts are typically installed before and after SCR catalysts, respectively. These materials are usually based on Pt and possess high activity for formaldehyde oxidation [47,48]. Even if some formaldehyde escaped oxidation and eventually formed HCN, the NH_3 slip catalyst could oxidize it prior to release to the environment. We have shown that Pd- and Pt-based catalysts abate HCN effectively above 300 °C [49], which is the temperature region where maximum levels of HCN were detected. Nonetheless, both formaldehyde and HCN can resist oxidation at lower temperatures, and therefore still represent a potential issue.

While mobile exhaust treatment systems are in principle already well designed to prevent HCN formation or emission, not all stationary systems are. Many stationary SCR installations function as standalone units directly downstream of the engine. Where operation conditions of the engine allow formation of formaldehyde in the exhaust gas, a catalytic oxidation system must be installed upstream of the SCR unit to avoid HCN formation.

Currently, HCN is not monitored in the exhaust of vehicles and stationary plants. However, legislations are constantly evolving [50], and it is recommendable to include HCN in the lists of regulated emissions due to its hazardous effects.

4. Conclusions

HCN can form in significant amounts during the SCR treatment of formaldehyde-containing exhaust gases over $V_2O_5/WO_3\text{-}TiO_2$. This undesired reaction not only lowers the SCR activity and consumes NH_3 parasitically, but also results in the production of a highly poisonous substance. While the detailed mechanism is not yet conclusive, we provide evidence that HCN production occurs from the direct reaction of formaldehyde and NH_3, and not through the formation of formic acid or ammonium formate. These results should serve as a basis for system designs and/or environmental legislation to prevent HCN emissions.

CRediT authorship contribution statement

Martin Elsener: Conceptualization, Methodology, Investigation, Writing - original draft, Formal analysis. **Rob Jeremiah G. Nuguid:** Writing - original draft, Formal analysis, Visualization. **Oliver Kröcher:** Supervision, Writing - review & editing. **Davide Ferri:** Conceptualization, Supervision, Writing - review & editing, Writing - original draft.

Declaration of Competing Interest

There are no conflicts of interest to declare.

Acknowledgments

The authors acknowledge the financial support from the Swiss National Science Foundation (SNF, Project #200021_172669/1).

Appendix A. Supplementary data

Supplementary material related to this article can be found, in the online version, at doi:https://doi.org/10.1016/j.apcatb.2020.119462.

References

[1] O. Kröcher, P. Granger, V.I. Pârvulescu (Eds.), Stud. Surf. Sci. Catal, vol. 171, Elsevier, 2007, pp. 261–289.
[2] I. Nova, E. Tronconi, Urea-SCR Technology for deNOx After Treatment of Diesel Exhausts, Springer, New York, 2014.
[3] Y. Ganjkhanlou, T.V.W. Janssens, P.N.R. Vennestrøm, L. Mino, M.C. Paganini, M. Signorile, S. Bordiga, G. Berlier, Appl. Catal. B 278 (2020) 119337.
[4] M. Koebel, M. Elsener, G. Madia, Ind. Eng. Chem. Res. 40 (2001) 52–59.
[5] M. Koebel, G. Madia, F. Raimondi, A. Wokaun, J. Catal. 209 (2002) 159–165.
[6] A. Russell, W.S. Epling, Catal. Rev. 53 (2011) 337–423.
[7] K. Kamasamudram, N.W. Currier, X. Chen, A. Yezerets, Catal. Today 151 (2010) 212–222.
[8] R. Nedyalkova, K. Kamasamudram, N.W. Currier, J. Li, A. Yezerets, L. Olsson, J. Catal. 299 (2013) 101–108.
[9] A.L. Marten, S.C. Newbold, Energy Policy 51 (2012) 957–972.
[10] M. Zhu, J.-K. Lai, I.E. Wachs, Appl. Catal. B 224 (2018) 836–840.
[11] A.R. Ravishankara, J.S. Daniel, R.W. Portmann, Science 326 (2009) 123–125.
[12] D. Zhang, R.T. Yang, Energy Fuels 32 (2018) 2170–2182.
[13] H.-Y. Chen, Z. Wei, M. Kollar, F. Gao, Y. Wang, J. Szanyi, C.H.F. Peden, J. Catal. 329 (2015) 490–498.
[14] F. Radtke, R.A. Koeppel, A. Baiker, Appl. Catal. A Gen. 107 (1994) L125–L132.
[15] F. Radtke, R.A. Koeppel, A. Baiker, Environ. Sci. Technol. 29 (1995) 2703–2705.

[16] H. Yasuda, T. Miyamoto, M. Misono, Reduction of Nitrogen Oxide Emissions vol. 587, American Chemical Society, 1995, pp. 110–122 ch. 9.
[17] I.O.Y. Liu, N.W. Cant, M. Kögel, T. Turek, Catal. Lett. 63 (1999) 214–244.
[18] I. Castellanos, O. Marie, Catal. Today 283 (2017) 54–65.
[19] I. Castellanos, O. Marie, Appl. Catal. B 223 (2018) 143–153.
[20] O. Kröcher, M. Elsener, E. Jacob, Appl. Catal. B 88 (2009) 66–82.
[21] D. Zengel, P. Koch, B. Torkashvand, J.-D. Grunwaldt, M. Casapu, O. Deutschmann, Angew. Chem. Int. Ed 59 (2020) 14423–14428.
[22] M.A. Elliott, G.J. Nebel, F.G. Rounds, J. Air Pollut. Control Assoc. 5 (1955) 103–108.
[23] S.M. Corrêa, G. Arbilla, Atmos. Environ. 39 (2005) 4513–4518.
[24] D.B. Olsen, C.E. Mitchell, J. Eng. Gas Turbine. Power 122 (1999) 611–616.
[25] M. Bauer, G. Wachtmeister, Mtz Worldw. Emagazine 70 (2009) 50–57.
[26] C.A. Harvey, R.J. Garbe, T.M. Baines, J.H. Somers, K.H. Hellman, P.M. Carey, SAE Transactions 92 (1983) 280–289.
[27] M.M. Baum, J.A. Moss, S.H. Pastel, G.A. Poskrebyshev, Environ. Sci. Technol. 41 (2007) 857–862.
[28] A. Marberger, M. Elsener, D. Ferri, O. Kröcher, Catalysts 5 (2015) 1704–1720.
[29] R.J.G. Nuguid, D. Ferri, A. Marberger, M. Nachtegaal, O. Kröcher, ACS Catal. 9 (2019) 6814–6820.
[30] A. Marberger, M. Elsener, R.J.G. Nuguid, D. Ferri, O. Kröcher, Appl. Catal. A Gen. 573 (2019) 64–72.
[31] M. Koebel, M. Elsener, M. Kleemann, Catal. Today 59 (2000) 335–345.
[32] S. Sun, J. Ding, J. Bao, C. Gao, Z. Qi, C. Li, Catal. Lett. 137 (2010) 239–246.
[33] C. Zhang, H. He, K.-i. Tanaka, Appl. Catal. B 65 (2006) 37–43.
[34] J.-K. Lai, I.E. Wachs, ACS Catal. 8 (2018) 6537–6551.
[35] C.G. Swain, A.L. Powell, W.A. Sheppard, C.R. Morgan, J. Am. Chem. Soc. 101 (1979) 3576–3583.
[36] S.D. Senanayake, D.R. Mullins, J. Phys. Chem. C. 112 (2008) 9744–9752.
[37] R. Zhang, H. Liu, B. Wang, L. Ling, J. Phys. Chem. C. 116 (2012) 22266–22280.
[38] M. Sridhar, D. Ferri, J.A. van Bokhoven, O. Kröcher, J. Catal. 349 (2017) 197–207.
[39] H.H. Richmond, G.S. Myers, G.F. Wright, J. Am. Chem. Soc. 70 (1948) 3659–3664.
[40] C. Chen, S.H. Hong, Org. Biomol. Chem. 9 (2011) 20–26.
[41] M.A. Sprung, Chem. Rev. 26 (1940) 297–338.
[42] N.E. Quaranta, J. Soria, V.C. Corberán, J.L.G. Fierro, J. Catal. 171 (1997) 1–13.
[43] G. Danger, F. Borget, M. Chomat, F. Duvernay, P. Theulé, J.C. Guillemin, L. Le Sergeant d'Hendecourt, T. Chiavassa, A&A 535 (2011) A47.
[44] A. Ćmikiewicz, A.J. Gordon, S. Berski, Struct. Chem. 29 (2018) 243–255.
[45] N. Aylward, N. Bofinger, Orig. Life Evol. Biosph. 31 (2001) 481–500.
[46] F.P. Cortolano, S.D. Pastor, R. Ravichandran, D.H. Steinberg, Tetrahedron Lett. 29 (1988) 5875–5876.
[47] C. Zhang, F. Liu, Y. Zhai, H. Ariga, N. Yi, Y. Liu, K. Asakura, M. Flytzani-Stephanopoulos, H. He, Angew. Chem. Int. Ed 51 (2012) 9628–9632.
[48] A. Gremminger, J. Pihl, M. Casapu, J.-D. Grunwaldt, T.J. Toops, O. Deutschmann, Appl. Catal. B 265 (2020) 118571.
[49] O. Kröcher, M. Elsener, Appl. Catal. B 92 (2009) 75–89.
[50] P. Bielaczyc, J. Woodburn, Emiss. Control. Sci. Technol. 5 (2019) 86–98.